Materials Science & Engineering B 229 (2018) 206–217

Contents lists available at ScienceDirect

Materials Science & Engineering B

journal homepage: www.elsevier.com/locate/mseb

Review

Semiconductor metal oxide gas sensors: A review

Ananya Dey

NMIMS Mukesh Patel School of Technology Management & Engineering, Mumbai, India

ARTICLE INFO

Keywords:
Types of gas sensors
Ammonia sensing
Semiconductor metal oxide
Sensitivity
Selectivity
Stability
Dopant induced variations

ABSTRACT

This review paper encompasses a detailed study of semiconductor metal oxide (SMO) gas sensors. It provides for a detailed comparison of SMO gas sensors with other gas sensors, especially for ammonia gas sensing. Different parameters which affect the performance (sensitivity, selectivity and stability) of SMO gas sensors are discussed here under. This paper also gives an insight about the dopant or impurity induced variations in the SMO materials used for gas sensing. It is concluded that dopants enhance the properties of SMOs for gas sensing applications by changing their microstructure and morphology, activation energy, electronic structure or band gap of the metal oxides. In some cases, dopants create defects in SMOs by generating oxygen vacancy or by forming solid solutions. These defects enhance the gas sensing properties. Different nanostructures (nanowires, nanotubes, heterojunctions), other than nanopowders have also been studied in this review. At the end, examples of SMOs are given to illustrate the potential use of different SMO materials for gas sensing.

1. Introduction

Detection and monitoring of flammable, toxic and exhaust gases are important for both energy saving as well as environmental protection [1,72]. Gas sensors have been in use for monitoring flammable as well as toxic gases in domestic and industrial environment [1]. The cheap, reliable, small and low power-consuming gas sensors are in great demand due to the wide range of applications. With the increasing demand for better gas sensors of higher selectivity and sensitivity, rigorous efforts are in progress to find more suitable material with required surface and bulk properties [13]. SMO gas sensors are generating interest as these materials fulfill the requirement of an ideal sensor to a very good extent.

Semiconductor metal oxide (SMO) gas sensors are the most investigated group of gas sensors [3] and recently the SMOs, having size in the range of 1 nm–100 nm, are being increasingly used for gas sensing due to their size dependent properties. Nanomaterials are unique because of their mechanical, optical, electrical, catalytic and magnetic properties. Apart from this, these materials also possess high surface area per unit mass. Further, new physical and chemical properties emerge when particles are in nanometer scale. The specific surface area as well as surface to volume ratio increase drastically when the size of the material decreases. Also, the movement of electrons and holes in semiconductor nanomaterials are affected by size and geometry of the materials [8]. High crystalline structure, ability of noble metal doping, and competitive production rate increase the demand of production for nanoparticles for gas sensors development [51].

This review article is focused on types of gas sensors and their comparison, factors affecting the sensitivity, selectivity and stability of SMO gas sensors, gas sensing mechanism of the above group of gas sensors. Furthermore the prospect of NH_3 sensing by different sensors are reviewed and compared with SMO gas sensors. Dopant or impurity induced variations which improve the properties of SMO materials for gas sensing applications is also being considered in this review.

2. Types of gas sensors

Over the past decades, many types of gas sensors have been developed based on different sensing materials and methods. Accordingly, the gas sensors are classified as catalytic combustion, electrochemical, thermal conductive, infrared absorption, paramagnetic, solid electrolyte and metal oxide semiconductor sensors [22]. Liu et al. [35] has classified the gas sensors based on their sensing methods and divided them to two groups: (a) methods based on variation in electrical properties and (b) methods based on variation in other properties. Materials like semiconductor metal oxides (SMO), carbon nanotubes and polymers are able to sense gas based on variation in electrical properties. The other variations are optic, acoustic, gas chromatographic and calorimetric. Comini [10] classified the gas sensors according to the measurement methods as (1) DC conductometric gas sensors (2) Field-Effect-Transistors (FET) based gas sensors (3) Photoluminescence (PL) based gas sensors. A comparison of various types of gas sensors is given in Table 1 and has been studied by Korotcenkov [29].

E-mail address: ananya.dey@nmims.edu.

https://doi.org/10.1016/j.mseb.2017.12.036
Received 31 July 2017; Received in revised form 22 November 2017; Accepted 27 December 2017
Available online 05 January 2018
0921-5107/

Table 1
Comparison of various types of gas sensors [29].

Parameters	Types of Gas Sensors				
	SMO Gas Sensors	Catalytic Combustion Gas Sensors	Electro Chemical Gas Sensors	Thermal Conductivity Gas Sensors	Infrared Absorption Gas Sensors
Sensitivity	E	G	G	P	E
Accuracy	G	G	G	G	E
Selectivity	F	P	G	P	E
Response Time	E	G	F	G	F
Stability	G	G	P	G	G
Durability	G	G	F	G	E
Maintenance	E	E	G	G	F
Cost	E	E	G	G	F
Suitability to portable instru-ments	E	G	F	G	P

E: excellent, G: good, F: Fair, P: Poor.

Though there are many types of gas sensors available, but in this study the focus will be on SMO gas sensors.

3. Performance of gas sensors

The performance of gas sensors can be evaluated by different parameters like sensitivity, selectivity, response time, [29,35], reversibility or recovery time [23,7,35] fabrication cost and stability [35]. Sensitivity is the smallest volume concentration of the target gas that can be sensed in the time of detection. Sensitivity can be defined as Ra/Rg for reducing gases and Rg/Ra for oxidizing gases, where Ra is the resistance of the gas sensor in the reference gas (usually air) and Rg stands for resistance of the sensor in the target gas [23,65]. This is unit less parameter and percentage sensitivity is expressed by [(Ra − Rg)/Ra] * 100% [45]. Selectivity is the ability of the gas sensors to detect a specific gas in a mixture of gases. Response time is the period from the time when gas concentration reaches a specific value to that when a sensor generates a corresponding signal. Reversibility is whether a sensor returns to its original state when gas concentration returns to normal [35]. Recovery time is the time required for a sensor signal to return to its initial value after a step concentration change from a certain concentration value to zero. Stability is the ability of a gas sensor to reproduce results for a certain period of time. The result includes retaining the sensitivity, selectivity, response time and recovery time. An ideal sensor should possess high sensitivity, selectivity and stability, low response time and recovery time and low fabrication cost [7].

The performance of the different materials (SMO, Catalytic metal, Conducting polymers, Optical sensors) can be compared with respect to their response time, and lower detection limit for a particular gas. In this section a comparative study is done to evaluate the performance of

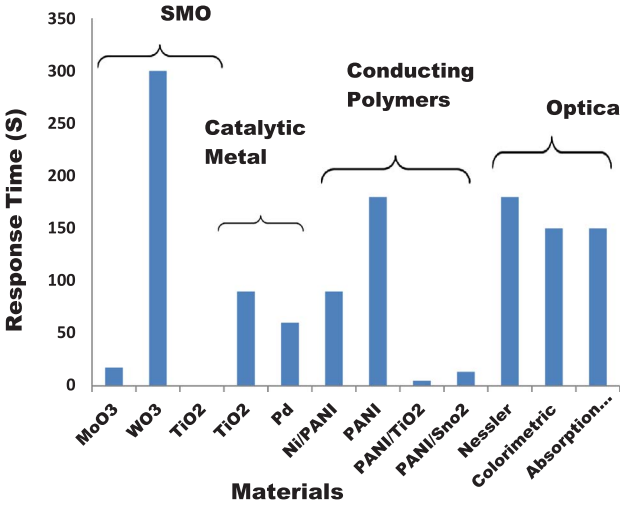

Fig. 1a. Comparison of different sensor materials according to their response time for NH_3 sensing [32,46,59,26,56,12,6].

SMO sensors with catalytic metal, conducting polymers and optical sensors, based on Ammonia (NH_3) sensing. NH_3 is included in this study as it is a natural gas that is present in the atmosphere in relatively low concentration of ppb or sub-ppb levels. Recently, most of the NH_3 is emitted by human activity. One of the major sources of NH_3 emission is combustion from chemical plants and motor vehicles. NH_3 sensors are used in food technology, chemical plants, medical diagnosis and environmental protection [46]. There are many ways to detect NH_3. High concentrations are easily detectable by penetrating odors. Gas sensors are required to determine lower concentration of NH_3. NH_3 sensors are applicable in automotive industry, chemical industry like fertilizer industry, refrigeration systems especially in ammonia production plant. NH_3 sensors are required in medical applications also. Measuring breath ammonia levels can lead to faster diagnostics for patients with urea imbalance due to different diseases [59]. Table 2 shows the requirement for NH_3 gas sensors in different application areas. Figs. 1a and 1b shows the comparison of different sensor materials with respect to their response time and lower detection limit for sensing ammonia (NH_3) gas and Figs. 2a and 2b show the comparison of different sensor materials with respect to their response time and working temperature, respectively, at different lower detection limits for ammonia (NH_3) gas sensing.

4. General properties of semiconductor metal oxide (SMO) used for gas sensing

The properties of SMOs can be divided into two groups according to the operating temperature which dictates the mechanism by which these materials function. The two groups are: (1) materials which follow surface conductance effects and (2) materials which follow bulk conductance effects. The first group of oxides operates at lower

Table 2
Requirements for ammonia gas sensors in different application areas [59].

Application		Detection limit	Required response time	Temperature range(°C)
Environmental	Monitoring ambient condition	0.1 ppb to > 200 ppm	Minutes	0–40
	Measure in stable	1 to > 25 ppm	~1 min	10–40
Automotive	NH_3 emission from vehicle	4- > 2000 g/min (conc. Unknown)	Seconds	Up to 300
	Passenger cabinet air control	50 ppm	~1 min	0–40
	NH_3 slip	1–100 ppm	Seconds	Up to 600
Chemical	Leakage alarm	20 to > 1000 ppm	Minutes	Up to 500
Medical	Breath analysis	50–2000 ppb	~1 min	20–40

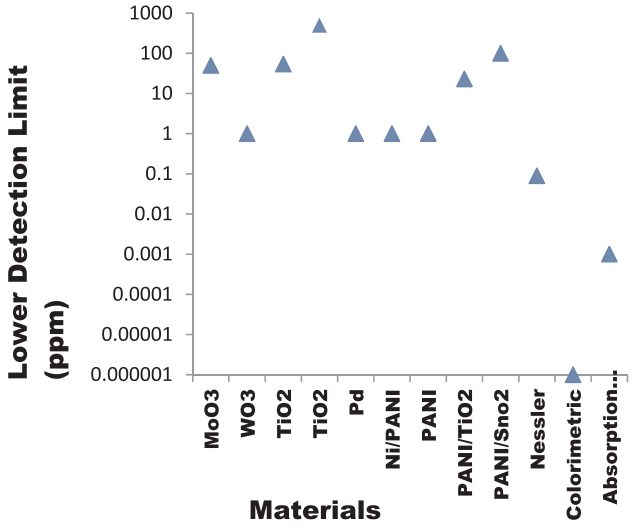

Fig. 1b. Comparison of different sensor materials according to their lower detection limit for NH_3 sensing [32,46,59,26,56,12,6].

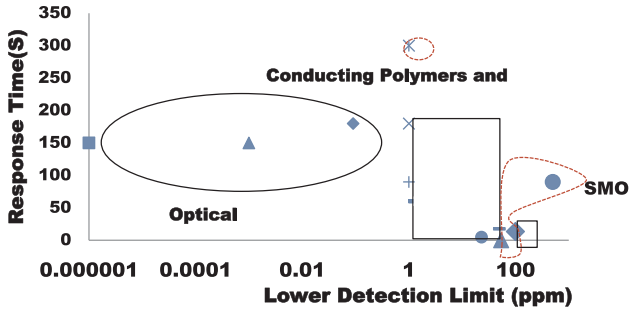

Fig. 2a. Comparison of different sensor materials according to their response time at lower detection limit for NH_3 sensing [32,46,59,26,56,12,6].

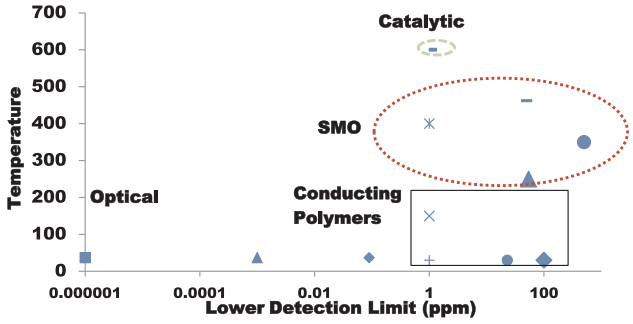

Fig. 2b. Comparison of different sensor materials according to their working temperature at lower detection limit for NH_3 sensing [32,46,59,26,56,12,6].

temperatures (400 °C–600 °C) and second group operates at high temperatures (> 700 °C) [42]. The metal oxide semiconductors which operate at low temperature, like SnO_2 and ZnO, are mainly called as surface conductance materials. At lower temperature the bulk defect effect is slow and conductance change is due to the formation and removal of surface oxygen. The bulk conductance materials respond to the changes in oxygen partial pressure in the upper temperature range (> 700 °C) and show the equilibrium between atmosphere and bulk stoichiometry. TiO_2, CeO_2, Nb_2O_5 are some of the examples of bulk conductance materials. The relationship between electrical conductivity and oxygen partial pressure of a metal oxide sensor is explained by the following equations [42]

$$\sigma = A \exp(-E_A/kT)\ p_o^{1/N} \quad (1)$$

where σ is electrical conductivity, A is constant, E_A is activation energy, k is the equilibrium constant, T is temperature and N is a constant depends on the bulk defects. If principal type of defect is doubly charged oxygen vacancy $V_{ö}$ occupying an oxygen site O^x, then equilibrium can be written as [42]:

$$O^x = V_{ö} + 1/2\ O_2 + 2e^- \quad (2)$$

Equilibrium constant can be written as:

$$k = [V_{ö}][e^2][p_o^{1/2}] \quad (3)$$

where [e] is the electron concentration.

Now, for balancing the charge,

$$[V_{ö}] = 2[e] \quad (4)$$

So, Eq. (3) becomes

$$k = [2e][e^2][p_o^{1/2}] \quad (5)$$

hence, [e] α $p_o^{-1/6}$, thus N = −6 for this type of defect. N value will vary if we assume other types of defect. The gas sensing mechanisms of these materials are explained in section 8.

5. Factors affecting the sensitivity of semiconductor metal oxide gas sensors

There are several technological methods available for optimization of sensor parameters. The sensitivity of the sensor can be increased significantly by changing the microstructure like grain size. For a large grain where D (grain size) ≫ 2L (thickness of the space charge layer), the conductance is limited by Schottky barrier at grain boundaries (known as grain boundary control). If D = 2L, conductance is limited by necks between grains (known as neck control) and if D < 2L, conductance is influenced by every grains (known as grain control) [7].

Another approach to improve the sensitivity is by changing the microstructure and porosity of the SMOs. Porous metal oxides with higher surface area exhibit increased gas sensitivity [7].

Sensitivity of the SMO gas sensors can be improved by the addition of dopants or impurities such as noble metals Pt [38,72], Nb [1], metal oxide PdO [69], and rare earth oxide CeO_2 [40]. The principles of working of additives modified metal oxide materials are not completely understood. However, mainly two mechanisms might be responsible for improvement of gas sensing. According to Bochenkov and Sergeev [7], first is a chemical scheme, mainly for spillover process and second is electronic mechanism.

Fig. 3 illustrates the three mechanisms of grain size dependence of conductance in semiconductor gas sensing materials. Thus the smaller grain size is better for the sensitivity of gas sensors, but excessive decrease in grain size decreases structural stability. A finely dispersed small crystallite has a deleterious effect on the temporal stability of the sensor [63].

Environmental humidity is an important factor for SMOs gas sensors. Increase in humidity reduces the sensitivity of metal oxide sensors [63].

6. Factors affecting the selectivity of semiconductor metal oxide gas sensors

One of the challenges for semiconductor metal oxide gas sensors is to achieve high selectivity. Generally two approaches exist for enhancing the selectivity of a SMO gas sensor. The first one is to synthesize a material which is selective to one compound and has very low or zero cross-sensitivity for other compounds which may be present in that working atmosphere. The second approach is to discriminate between several analytes in the mixture. This is usually achieved by either modulation of temperature [7] or by using sensor arrays [7,35].

Addition of dopants or impurities to the metal oxides or synthesis of

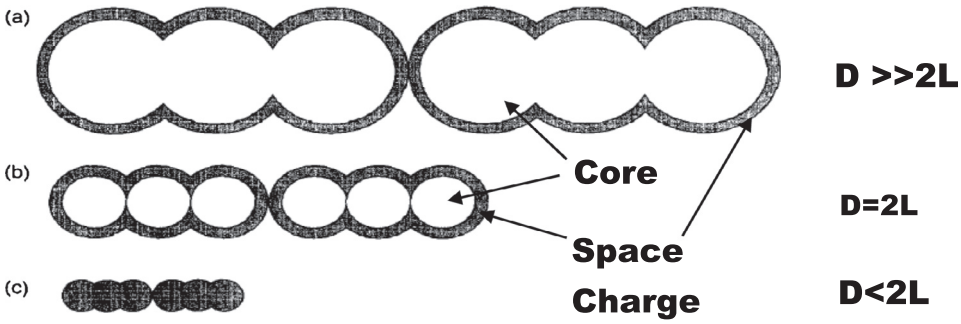

Fig. 3. Three mechanisms of grain size dependence of conductance in semiconductor gas sensing materials (a) D ≫ 2L, grain boundary control (b) D = 2L, neck control (c) D < 2L, grain control [7].

mixed metal oxides also enhances the selectivity of the gas sensors as each material is selective to specific gas species. Dopants/impurities improve the quality and performance of the sensors [58].

7. Factors affecting the stability of semiconductor metal oxide gas sensors

Stability is one of the key parameters in the development of gas sensors for the real market as the sensors should produce a stable as well as reproducible signal at least for 2–3 years which corresponds to 17,000 h–26,000 h of operation [30]. Low stability is an issue with SMO materials. Sensor stability can be of two types. One is related to the reproducibility of the sensor characteristics during a certain period of time at working conditions including high temperature and presence of a known analyte. Such stability is referred to as active stability. The other stability is connected with retaining the sensitivity and selectivity during a period of time at normal storage conditions like room temperature and ambient humidity. According to Korotcenkov and Cho [30] the factors which might be responsible for instability are structural transformation, phase transformation, poisoning, degradation of contacts and heaters, bulk diffusion, error in design, change in humidity, fluctuations of temperature in the surrounding atmosphere and interference effect. There is no uniform approach to increase stability of the metal oxide sensors. Stability can be increased to some extent by calcination and annealing as the post processing treatment and by reducing the working temperature of the sensing element. Doping metal oxides with other metals or synthesis of mixed oxides also increase the stability of the sensor elements [7].

Improvement of engineering approaches like drift compensation, selecting a correct gas system components, incorporating additional filters and temperature stabilization can also eliminate the problems of sensor stability [30].

8. Gas sensing mechanisms of semiconductor metal oxides

The gas sensing mechanism of SMO sensors involves two major functions - receptor and transducer. The receptor function involves recognition of a target gas in gas - solid interface, which includes electronic change in the surface of the metal oxides. Transducer function involves transduction of the surface phenomenon into an electrical resistance change in the sensors [67,15,25]. Fig. 4a shows both receptor and transducer functions.

According to Korotcenkov and Cho [30], chemical properties of the surface oxygen of the oxide itself is responsible for the receptor function in a neat sensor device as this function is responsible for the ability of the surface oxide to interact with the target gas. This function can be modified when the oxide surface is loaded with additive (noble metal, acidic and basic oxide). Change in receptor function induces a large change in sensitivity. Transducer function is responsible for converting the signal caused by chemical interaction of the oxide surface (change in work function) into electrical signal. This function is dominated by each boundary between grains. Fig. 4b illustrates receptor function and transducer function as well as physicochemical and material properties involved for semiconductor gas sensors.

The gas detection in SMO gas sensors are related to ionosorbed surface oxygen and target analyte gas. There is a shift in the state of equilibrium of the surface oxygen reaction due to the presence of target analyte gas. This is called transducer function. The resulting change in chemisorbed oxygen changes the conductivity of the SMO materials [48]. This is called transducer function. Fig. 4c illustrates the receptor and transducer functions along with parameters influencing sensor performance.

Fig. 5 shows the gas sensing mechanism of undoped and Co-doped ZnO thin films for NH_3 gas.

8.1. Electron depletion

The SMOs used as gas sensor materials, are crystalline in nature and they are connected to their neighbouring grains by necks. These interconnected grains form larger aggregates which are connected to their neighbours by grain boundaries. On the surface of the grains, the adsorbed oxygen molecules extract electrons from the conduction band and trap the electrons at the surface as ions, which produces a band bending. As a result, an electron depleted layer is formed which is called as space-charge layer. When the particle size of the sensing film is close to or less than twice the thickness of the space-charge layer, the sensitivity of the sensor will increase [55]. The relation between grain size and sensitivity is already discussed in section 5. The donor or acceptor gaseous electrons are adsorbed on the metal oxide surface and exchange electrons with the SMO sensors. An acceptor molecule will extract electron from the SMO sensors and decrease its conductivity, whereas there will be an increase in conductivity for a donor molecule. The overall conductivity of a metal oxide semiconductor gas sensor depends on the charge transfer mechanism between adsorbed gaseous species and semiconductor metal oxides and the analyte gas surface reaction [20]. Thus the gas sensing mechanism of a SMO gas sensor is based on the gas/semiconductor surface interaction. This interaction occurs at the grain boundaries of the polycrystalline metal oxides. The processes taking place in metal oxide during gas detection include reduction/oxidation processes of the semiconductor, adsorption of the chemical species directly on the semiconductor, electronic transfer of delocalized conduction-band electrons to localized surface state and vice versa, catalytic effects and complex surface chemical reactions between the different adsorbed chemical species [29].

8.2. Band bending

When a sensor is heated to a high temperature, free electron flows easily through grain boundaries of SMO films. In an oxygen atmosphere, oxygen is adsorbed at the semiconductor metal oxide surface which forms a potential barrier at the grain boundary. The interaction of atmospheric oxygen with the SMO surface forms a layer of charged oxygen species, which traps electrons from the bulk of the materials. The layer of charged oxygen species repels other electrons from

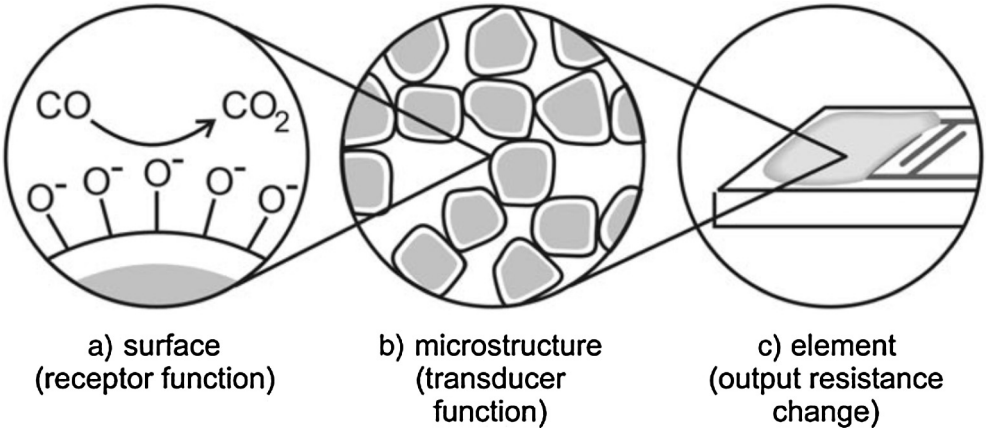

Fig. 4a. Receptor and transducer functions of metal oxide semiconductor gas sensor [15].

interacting with the bulk of films, creating a region depleted of electrons and increasing the potential barrier at the grain boundaries. This restricts the flow of electrons and increases the resistance [25]. Below a temperature 147 °C, oxygen is ionosorbed as O_2^- and it is ionosorbed as O^- between temperatures 147 °C to 397 °C, which is mainly the operating temperature of the gas sensors. Above 397 °C formation of O^{2-} occurs. The required electrons for this process originate from the donor site which has intrinsic oxygen vacancies. These electrons are extracted from the conduction band and trapped at the surface leading to an electron depleted layer called as space charge layer $\hat{}_{Air}$. The presence of negative surface charge leads to band bending which generates a potential barrier at the surface $eV_{surface}$. The height ($eV_{surface}$) and the depth ($\hat{}_{Air}$) depends on the charge of the surface which depends on amount and type of adsorbed oxygen [15]. Figs. 6a and 6b show the band diagram of metal oxide semiconductor after chemisorption of charged species (ionosorption of oxygen).

E_F, E_C and E_V are the energy of the Fermi level, conduction band and valence band, respectively. Positive Charge is donor site and e- are conducting electron.

8.3. Resistance change

The surface of the semiconductor metal oxide adsorbs the gas molecules in case a sensor is exposed to a reducing gas. Adsorption of a gas molecule on the surface reduces the potential barrier by injecting electrons to the conduction band, allowing the electron to flow easily and thus reducing the electrical resistance. In this manner, the SMO gas sensors act as variable resistors whose value is a function of gas concentration [25]. The response to reducing gases may be from reactions involving the consumption of the surface oxygen ion and replenishment of the charge carrier density on the conduction band of the n type semiconductors, which is shown by reaction 6 [42]. The reverse phenomenon occurs during the exposure to oxidizing gases. In the case of n-type semiconductor, the resistance of the gas sensors decreases when they are in contact with reducing gases or vapors [13].

$$O^-_{2sur} + 2CO = 2CO_2 + e^-_{bulk} \quad (6)$$

O_{2sur}^- is surface oxygen ions and e_{bulk}^- is electrons in bulk materials. The response for the oxidizing gases will be just the opposite. This behaviour also correlates with oxygen partial pressure. Table 3 shows

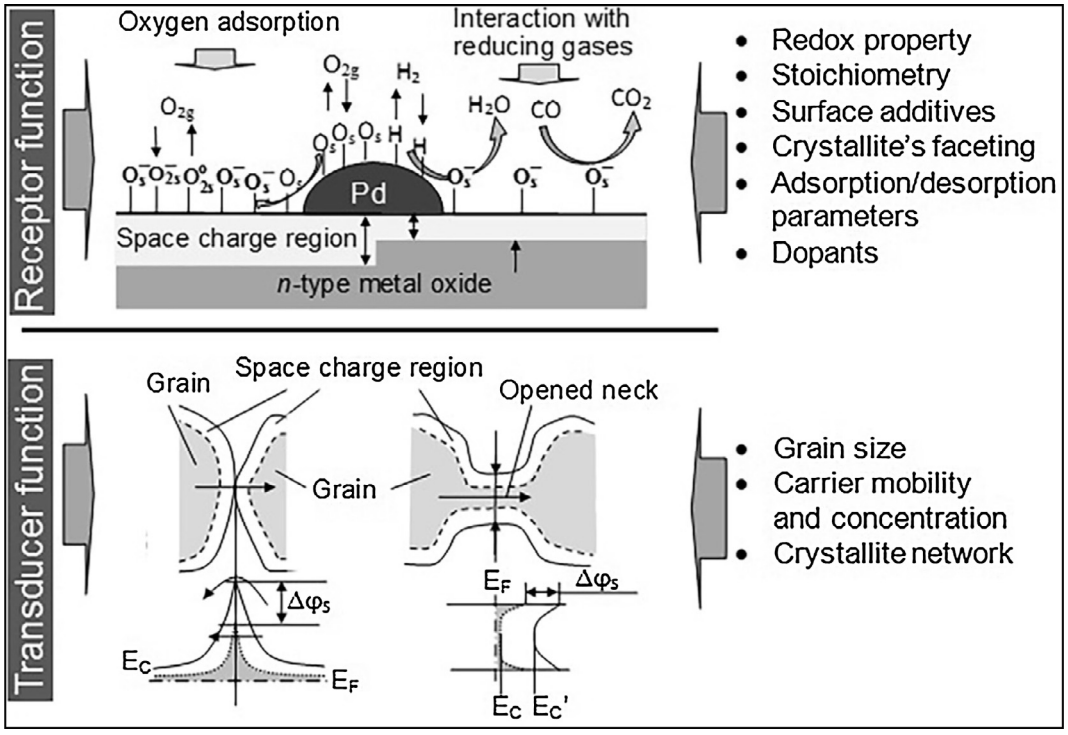

Fig. 4b. Receptor and transducer functions as well as their physicochemical and material properties of metal oxide semiconductor gas sensor Korotcenkov and Cho [30].

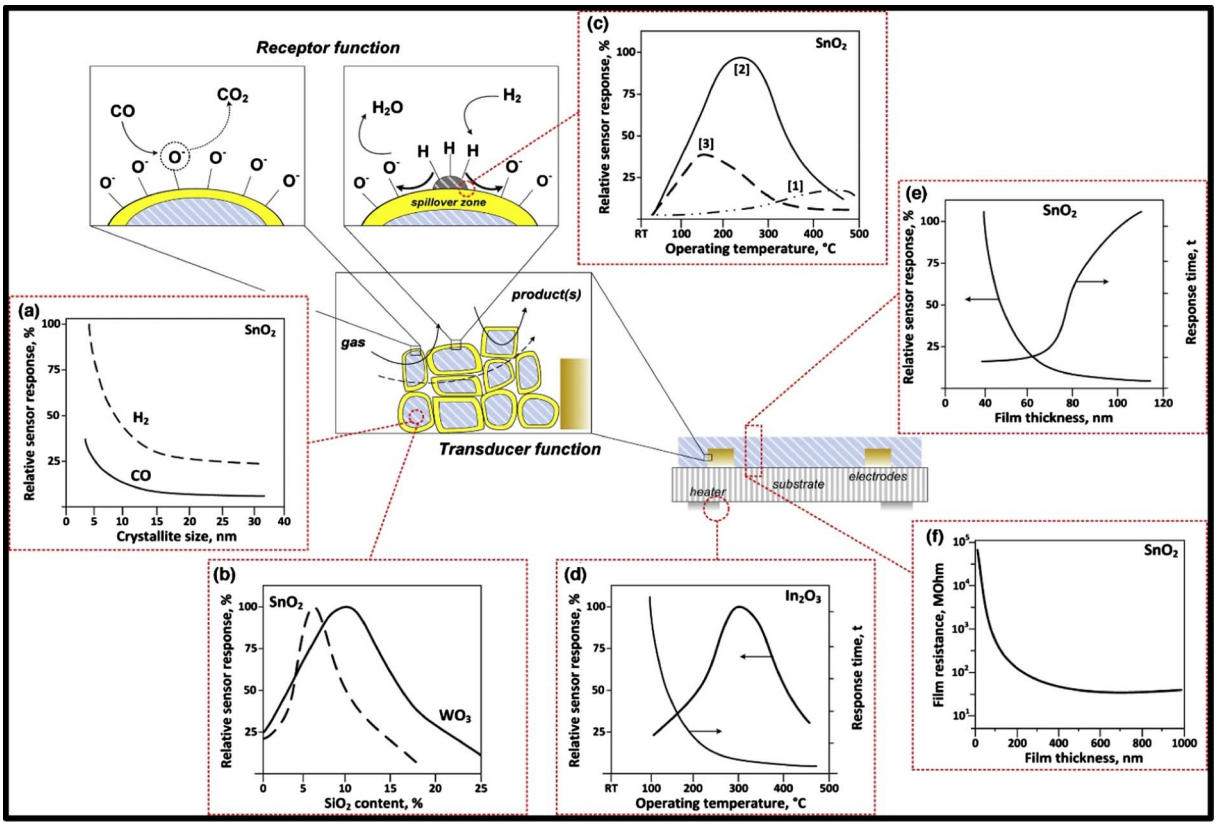

Fig. 4c. Receptor and transducer functions of metal oxide semiconductor gas sensor (a) SnO_2 sensors response as a function of crystal size (b) SnO_2, WO_3 sensor response as a function of SiO_2 content (c) Influence of Pd (d) influence of operating temperature on In_2O_3 on sensor response and response time (e) Influence of SnO_2 film thickness on sensor response and response time (f) SnO_2 film resistance [48].

the sign of resistance change (increase/decrease) for change in gas atmosphere.

For N-type gas response, conductivity will increase in presence of reducing gas whereas for P-type response, conductivity will decrease in presence of reducing gas. Many binary oxides with band gap 2–4 eV like TiO_2, Nb_2O_5, Ta_2O_5, ZnO, SnO_2, MoO_3 and WO_3 exhibit n-type behaviour in response to the introduction of minority gases in an air ambient. Other binary oxides such as NiO, CuO, Cr_2O_3, Co_3O_4 and Mn_3O_4 exhibits p-type gas sensing characteristics. Some oxides switch between n-type and p-type gas response under the relevant set of conditions (temperature, oxygen partial pressure, presence of relatively small concentration of foreign gas in air ambient). Both n-type (MoO_3) and p-type (CO_3O_4) semiconductor metal oxides can exhibit good gas sensing properties at different temperature [43].

The ammonia vapour sensing mechanism by metal oxide thin film surface can be explained by the following equations [39]:

$$O_2 + e^-_{(SMO\ surface)} = O^-_{2(SMO\ surface)} \quad (7)$$

$$4NH_3 + O_2^{-(ad)=} 2N_2 + 6H_2O + 6e^- \quad (8)$$

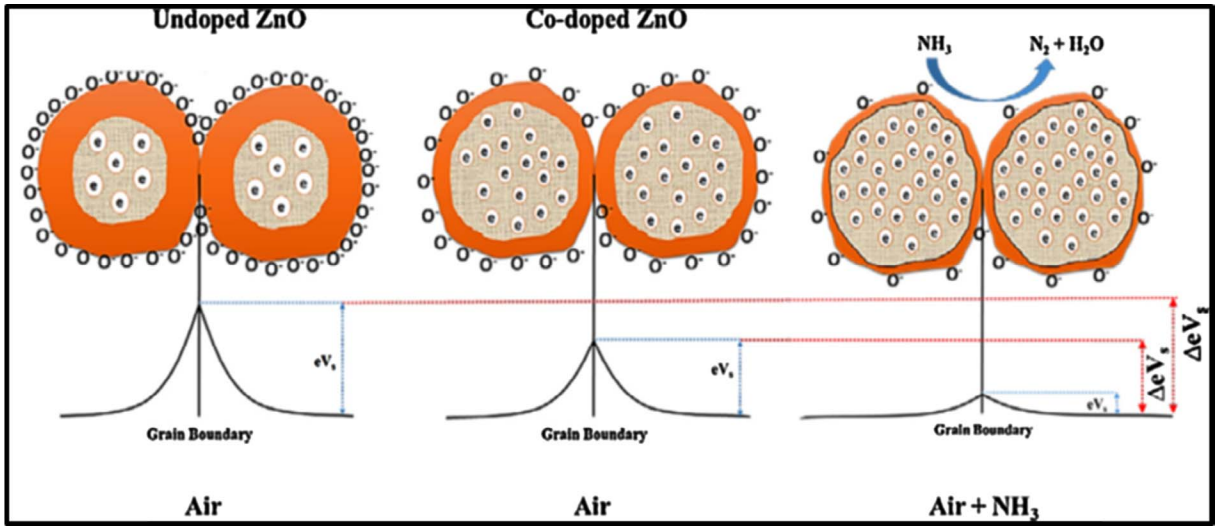

Fig. 5. Schematic diagram of undoped ZnO and Co-doped ZnO thin films for Ammonia Gas sensing [39].

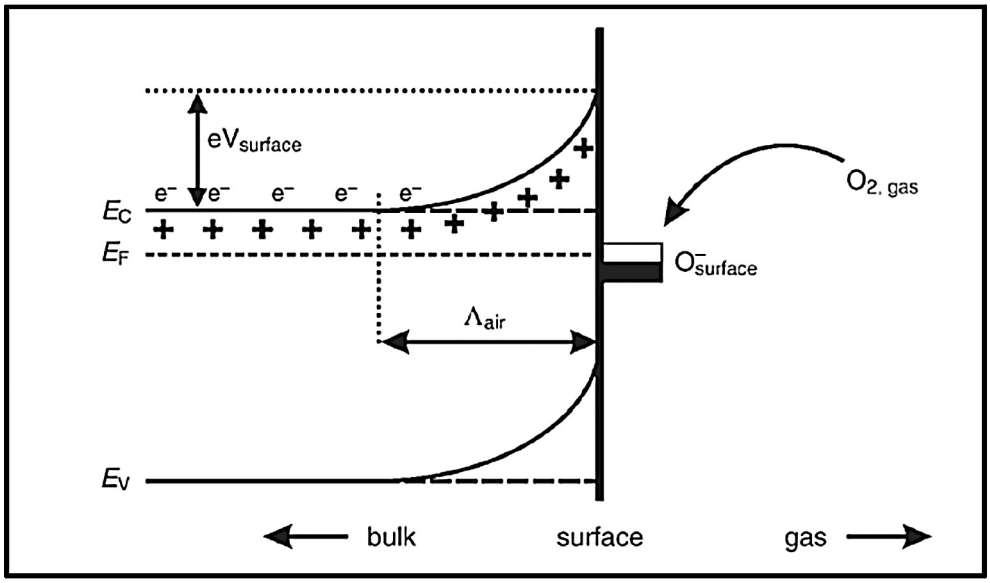

Fig. 6a. Band diagram of n-type semiconductor metal oxide surface after chemisorption of oxygen [15,63].

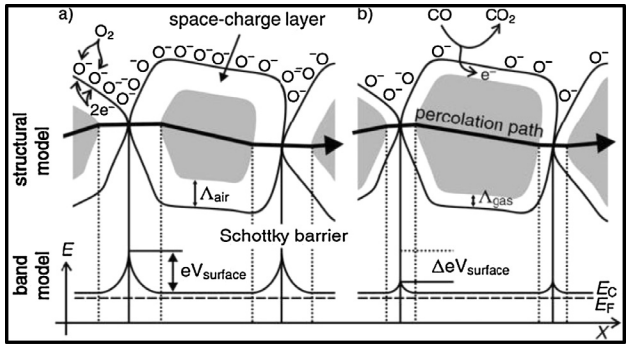

Fig. 6b. Structural and band model for conductive mechanism of a polycrystalline metal oxide semiconductor (a) initial state (b) effect of CO [15,63].

Table 3
Resistance change for change in gas atmosphere [66,14].

Classification	Reducing Gas	Oxidizing Gas	Decrease in Oxygen Partial Pressure
n-type	Resistance decrease	Resistance increase	Resistance decrease
p-type	Resistance increase	Resistance decrease	Resistance increase

9. Dopant/impurity induced enhancements of the properties of semiconductor metal oxide for gas sensing applications

Doping during synthesis and deposition process influence those metal oxide properties which are important for gas sensing applications. The parameters like sensitivity, selectivity, response time and stability of the gas sensors are improved by addition of different dopants [50]. In some cases, dopants are added to a metal oxide to modify its properties by enhancing the desirable properties, while in other cases undesirable properties are reduced or eliminated [54]. Even though SMO gas sensors are catalytically active, a small amount of catalytically active metals or metal oxides are often added to it for improving the selectivity and sensitivity of the sensors [13]. For example, the surface modification by noble metals promotes the improvement in sensitivity and decrease in response and recovery times. The metal oxide doping by transition metal modifies the catalytic reactivity and morphology of deposited films.

There are different mechanisms which are followed by dopants/impurities to enhance the properties of nanoparticles metal oxides like (1) change in microstructure and morphology, (2) formation of stoichiometric solid solution, (3) change in activation energy, (4) generating oxygen vacancy, and (5) change in electronic structure.

9.1. Change in microstructure and morphology

Microstructure and grain size are the two most influential factors in sensing properties of semiconductor gas sensors. Sensor response increases drastically when grain size decreases [69]. Anukunprasert et al. [1] reported that there is a sharp increase in sensitivity as the grain size becomes smaller than the space-charge depth. The relationship of grain size and sensitivity is discussed in section 5. Addition of dopants can inhibit particle growth. Maciel et al. [37] reported that the reduction in particle growth rate at high temperatures can be controlled by using dopants. Also a Ce-rich surface layer is responsible for the increase in the thermal stability and particle growth inhibition of the nanoparticles. The experimental results showed that Ce could be used to control particle size of SnO_2. The researchers also showed that Ce stabilizes SnO_2 nanoparticles against particle size growth at temperature range from 550 °C to 1100 °C. In TiO_2–CeO_2 mixed oxide, the phase composition and Crystalline size depends upon Ce:Ti molar ratio. TiO_2-CeO_2 can be used for sensing CO at low operating temperature and has a potential use in industrial application [40]. Nb-doped TiO_2 also inhibited the grain growth [1].

9.2. Formation of stoichiometric solid solution

Solid solutions can be formed by the dopants and the host metal oxides. Dopants can either form solid solution by substitution of the host atoms from the lattice or these can be interstitially present in the host lattice. Interstitially dissolved foreign atoms may change the strain in the lattice and, when ionized, their charge affects the electro neutrality condition while the substitutionally dissolved impurities or dopants also change the properties of metal oxides if their charge or size is different than the host atoms. Thermal stability is improved and particle growth can be inhibited by formation of a solid solution between SnO_2 and dopants like rare earth oxides (Y_2O_3, La_2O_3 and CeO_2) [37]. It is reported that the particle growth is controlled by the motion of boundaries between the particles. The mean boundary velocity is given by the following formula

$$V = M\Delta F \quad (9)$$

where M is the particle boundary mobility which is a kinetic parameter and depends on the mechanism of diffusion, ΔF is thermodynamic driving force; the mean boundary velocity can be reduced by reducing the above two factors. Both the factors can be reduced by forming metastable solid solution which develops a segregation layer of foreign cations on the particle surface. This cation rich surface layer inhibits particle growth and improves thermal stability. Also the formation of this layer contributes towards reduced surface mobility and decreased surface energy (acting in the driving force) [33]. The linear relationship with lattice parameter and dopant concentration indicates the formation of solid solution. In case of solid solution Ce^{4+} substitute Ti^{4+} in the lattice and as a consequence, the unit cell parameters change [41].

Maciel et al. [37] reported that lattice parameters c/a ratio of Ce-doped SnO_2 is greater than pure SnO_2. This is because of the formation of stoichiometric solid solution by substitution of the Sn^{4+} (0.71 Å diameter) by Ce^{4+} (0.92 Å diameter) in the Crystalline. Growth rate of Ce-doped SnO_2 are also smaller than undoped SnO_2.

In a stoichiometric solid solution, the dopant cations acts as acceptor centers if their charge is less than the cations they replace, and act as donor centers if their charge is greater than the cations they replace [54]. In this solid solution, an extra negative charge can be compensated either by an oxygen vacancy or a cation interstitial, given by the following equations:

(2MO)

$$A_2O = 2A_M^{/} + O_o + V_{\ddot{o}} \quad (10)$$

(MO)

$$A_2O = A_M^{/} + A_{\dot{i}} + O_o \quad (11)$$

where MO is the host metal oxide of a divalent metal, while A^+ and D^{3+} acceptor and donor dopant cations [54].

In a stoichiometric solid solution an extra positive charge can be compensated by either a cation vacancy or oxygen interstitial given by the following equations [54]

(2MO)

$$D_2O_3 = 2\dot{D}_M + O_o + O_I^{//} \quad (12)$$

(3MO)O

$$D_2O_3 = 2\dot{D}_M + V_M^{//} + 3O_o \quad (13)$$

9.3. Change in activation energy

The resistance of TiO_2 is dependent on conduction mechanism which is related to oxygen partial pressure. The relationship can be expressed by following formula [72]:

$$R = AP_{O2}^{-1/m}\exp(E/kT) \quad (14)$$

where R is resistance, A is a constant, Po_2 is oxygen partial pressure, E is activation energy, k is Boltzmann constant, T is temperature and m is a constant dependent on the defects. Taking natural logarithm on both sides:

$$\ln R = \ln A + E/kT - 1/m \ln Po_2 \quad (15)$$

If $Po_2 = 1$, at two different temperatures, the Eq. (13) becomes:

$$E = k(T_i * T_2)/(T_i - T_2) * (\ln R_1 - \ln R_2) \quad (16)$$

where R_1 and R_2 are the sensor response at different temperature T_1 and T_2.

The relation between sensor response and activation energy can be explained as the gas approaches the surface of the material, they absorb energy and become activated. Then they react with the particles (may be some dopants) absorbed at the surface of the material by following reaction:

$$r = C\exp(-E/kT) \quad (17)$$

where r is rate of reaction and C is pre- exponential factor. Reaction rate constant increases as activation energy decreases. Thus, rate of response of the sensor becomes higher by lowering activation energy. Some dopants (like platinum) have notable effect on activation energy. Platinum also provides active sites for incoming gases which is called spill-over effect [72]. So, doping SMOs with platinum can also enhance sensitivity of the gas sensors.

9.4. Generating oxygen vacancy

Oxygen vacancies are considered to be important reactive agents for many adsorbates. So, many surface reactions are influenced by this type of point defect. Oxygen vacancy acts as direct adsorption site as well as electron donor site. Further, oxygen vacancies act as nucleation centre for small metal clusters (example Au) [64]. The formation and annihilation of oxygen and variation in O-vacancy concentration as a function of oxygen chemical potential is an important mechanism for gas sensors [4]. Doping with a second element will have a significant effect for the metal oxides which are dominated by defect chemistry (via oxygen vacancy). Oxygen vacancy is a major advantage for some metal oxide like Titania [50] and CeO_2 [41].

Doping TiO_2 with aluminum generates oxygen vacancy and increases the conductivity of TiO_2. Aluminum may dissolve substitutionally by occupying a regular cation position in the TiO_2 lattice as their ionic radii are similar (0.074 Å for Ti^{4+} and 0.067 Å for Al^{3+}). In the lattice of TiO_2, aluminum will remain present as a defect with single negative charge [53].

$$Al_2O_3 = 2Al_{Ti}^{/} + 3Ox + V_{\ddot{o}} \quad (18)$$

The presence of oxygen vacancy will increase the conductivity of the solid. If there is low oxygen partial pressure, then generation of more oxygen vacancies are expected

$$TiO_2 = Ti_{Ti} + V_{\ddot{o}} + 1/2\ O_2 + 2e\ [10] \quad (19)$$

The generation of oxygen vacancy which is related to the lattice defect will be determined by factors like ionic radii (large cation/anion may not fit in the available interstitial lattice site) and charge on the defect [54]. In aluminum doped TiO_2, the crystalline size and particle size increase initially with 5 wt% of aluminum followed by a decrease with 7.5 wt% aluminum. Al-doped TiO_2 sensors are more sensitive and selective to oxygen and carbon monoxide at a temperature around 600 °C than pure TiO_2 sensors [9].

The n-type behaviour of SnO_2 associated with the oxygen deficiency in the bulk is shown in the Fig. 7. Donors are singly ionized and doubly ionized oxygen vacancies for SnO_2 bulk materials. Donor levels (ED1 and ED2) are located at 0.03 and 0.15 eV below the conduction band edge.

9.5. Changes in electronic structure/band gap

The gas sensor materials can be divided into two types as (1) bulk sensitive (2) surface sensitive depending on the change in conductivity upon exposure to different gases. TiO_2 when acts as bulk sensitive material, exhibits conductivity change mainly due to formation of O-vacancy and Ti interstitials [4]. SnO_2 and ZnO are the examples of surface sensitive materials which show the change in conductance mainly due to band bending. The adsorption of charged surface oxygen species plays an important role in sensing oxidizing and reducing gases in case of surface sensitive metal oxides. The negatively charged surface oxygen species introduce a band bending in upward direction which reduces the charge carriers in the conduction band thus causing a drop in conductivity. The concentration of the charged oxygen species depends on the equilibrium with the gas phase. The reducing gases react with these pre-adsorbed oxygen species and reduce their concentrations thus increasing the conductivity of the gas sensors [4]. The surface conductivity depends on density of the donors (adsorbed hydrogen

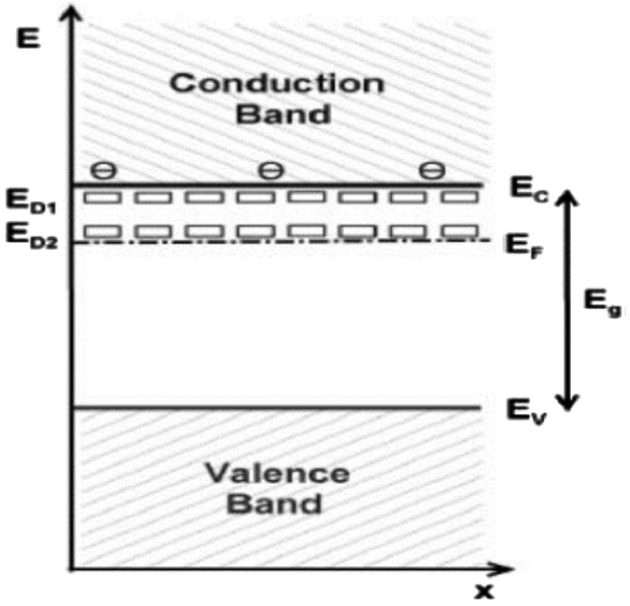

Fig. 7. Schematic band diagram of SnO2 bulk. Two vacancy donor level are located at two donor levels 0.03 and 0.15 eV below the conduction band [62].

atoms and oxygen vacancies) and acceptors (chemisorbed oxygen) [13]. It is also reported by Zhan et al. [71] that for tin oxide band bending effect is considered as the main mechanism for gas sensing, in a semiconductor metal oxide the best way to describe the conduction process is by considering the free charge carriers (electron/hole) must overcome the intergranular barriers that result from band bending at the adjacent surface of the neighboring grain due to formation of the Schottky barrier at grain boundaries of the particles [71]. Krunagaran et al. [26] proposed the reduction of surface oxygen as the dominant mechanism for increase in conductance of TiO_2 on exposure to ammonia.

It is evident from the literature that a single metal oxide used as functional material always has some disadvantages. Addition of dopants or impurities improves the properties of SMOs. Fig. 8 illustrates the change in band gap when ZnO is doped with CO.

10. New SMO nanostructures as gas sensor

Last two decades nanostructures like nanowires, nanotubes, core-shell nanostructures, nanoneedle, nanosheets, and nanofibers have emerged as future electronic devices for their large surface to volume ratio. Recently SMO nanowires are extensively studied to detect toxic gases. The gas sensing properties of SMO-nanowires are higher than their bulk or thin film counterparts [24]. But, nanowire sensors are not commercially available [11]. Table 4 summarizes different nanostructures (other than nanoparticles) of SMOs which can be used in gas sensing applications.

Table 4
Different SMO nanostructure for gas sensing.

Morphology	SMO	Gas	Reference
Nanowire	NiO	Ethanol, Acetone (500 °C)	Kaur et al. [27]
Nanowire	WO_3	H_2S	Krainer et al. [31]
Nanowire	ZnO, CuO	Ethanol	Zappa [70]
Nanotube	TiO_2	Co, Acetone, Ethanol (400 °C, 500 °C)	Galstyan et al. [16]
Core-Shell nanostructures	TiO_2-CuO	NO_2	Park et al. [44]
Nanosheets	CuO	Acetone, methanol, ethanol (200 ppm, 340 °C)	Umar et al. [61]

Table 5 gives a summary of the previous studies of nanoparticle SMO materials for gas sensing, arranged chronologically.

11. Conclusion

A study on semiconductor metal oxide gas sensors has been exhibited in this review. It is an attempt to bring out a comparative study of different types of gas sensors with SMOs. General properties and gas sensing mechanisms of SMOs are also discussed in detail. Moreover, a comprehensive study has also been done on factors that are affecting the sensitivity, selectivity and stability of the semiconductor metal oxide gas sensors. The study establishes that the dopants or impurities enhance the gas sensing properties of SMOs by any of the processes such as changing the microstructure or morphology, forming stoichiometric solid solution, changing the activation energy, generating oxygen vacancy or changing the electronic structure/band gap. It is observed that recent developments in SMO nanostructures (nanowires, nanotubes, core-shell nanostructures, nanoneedle, nanosheets, and nanofibers) is paving the way for newer and better gas sensor materials. Further studies can be carried out to give added information on dopant induced variations of SMOs for gas sensing.

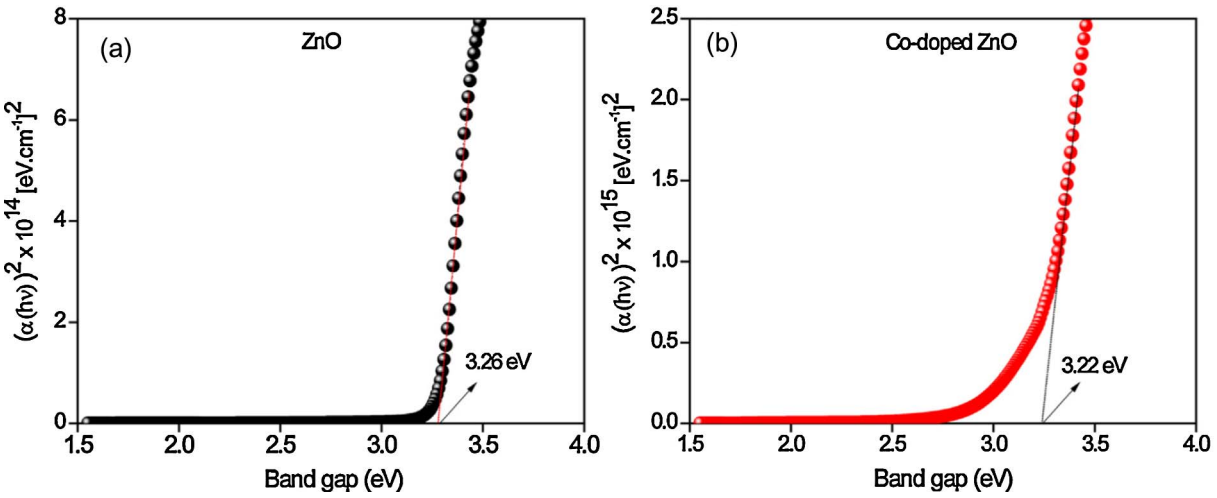

Fig. 8. Band gap energies for (a) undoped ZnO (3.26 eV) (b) Co-doped ZnO (3.22 eV) [39].

Table 5
Summary of studies of nanoparticle SMOs for gas sensing.

Nano particles	Properties of Nanoparticles	Synthesis Technique	Fabrication Technology	Sensing Gas	Author
TiO_2	Size: 3 nm–30 nm	Chemically modified sol-gel technique	Dip-coating technique	Ethanol (100 ppm), Methanol (100 ppm), CO (100–300 ppm) NO_2 (0.5–4 ppm) Temperature = 400 °C and 500 °C RH = 30%	Garzellaet al. [17]
SnO_2	Size: 40 nm	NR*	Screen-printing	NH_3 (937.5 ppm) Temperature = 104 °C–480 °C RH** = 20%	Llobetet al. [36]
CeO_2-TiO_2	NR*	Sol–gel	Spin-coating technique	O_2 (10,000 ppm) Temperature = 420 °C RH = < 5%	Trinchiet al. [60]
SnO_2	Size: 17.8 nm	Aerosol flame reactor (Premixed Flame)	Thick film deposition by drop coating method	NO_2 (10–5000 ppb) Propanol (10–300 ppm) CO (500–10,000 ppm) Temperature = 200 °C–400 °C RH = 50%	Sham et al. [51]
Nb-doped TiO_2 (3%–5%)	Size:10–15 nm Specific area: 70–80 m^2/g	Water – in-oil micro emulsion technique	Thick-film sensor	CO (1000 ppm) Temperature = 650 °C RH = NR*	Anukunprasert et al. [1]
F-doped SnO_2	Size: 12–15 nm (calcinated at 550 °C) Surface area: 70 m^2/g	Sol-gel	Micro-electro mechanical system (MEMS)	CO, H_2, C_3H_8, CH_4 (100–600 ppm) Temperature = 22 °C, RH = 50%	Han et al. [21]
TiO_2	Size: 15 nm	NR*	Micro-electro mechanical system, nanoparticles deposited spin coating	Methanol (50 ppm) Temperature = 375 °C–475 °C RH = dry air	Benkstein et al. [5]
Pt/SnO_2	Size: 10 nm	Flame spray pyrolysis (FSP)	In-situ deposition	CO (8–50 ppm) Temperature = 350 °C RH = dry air	Madler et al. [38]
TiO_2	Surface area:36–103 m^2/g Size: 5–43 nm	Flame-spray Pyrolysis	Drop-coating method	Isoprene, ethanol, Acetone and CO (1–75 ppm) Temperature = 500 °C RH = dry air	Telekiet al. [57]
Al-doped TiO_2 (5–7.5 wt%)	Size:53 nm–76 nm	Citrate–Nitrate auto combustion method	NR*	CO (100–500 ppm) Temperature = 600 °C RH = dry air	Choi et al. [9]
TiO_2	NR*	NR*	DC reactive magnetron sputtering	NH_3 (500 ppm) Temperature = 250 °C	Karunagaran et al. [26]
TiO_2	Ave size: 10 nm	Novel chemical route	Matrix assisted pulsed laser evaporation (MAPLE)	VOC (ethanol, acetone, 20–200 ppm) Temperature = 250 °C–500 °C, RH = dry air	Rella et al. [47]
CuO	NR*	Thermal deposition method	NR*	NO_2 (200 °C)	Li et al. [34]
Tungsten trioxide (WO_3)	Lamellar structured with diameter: 100–350 nm, thickness 20–50 nm, Specific surface area: 7–19 m^2/g	Acidification method	Nanoparticle paste is screen-printed on an alumina substrate equipped with a pair of comb-type Au microelectrode	NO_2 (50–1000 ppb) Temperature = 200 °C RH = dry air	Kida et al. [28]
Tungsten trioxide (WO_3) nanotubes	200 nm pore diameter & 600 nm pore length. Single nanotube is formed by discrete grain size of 60–80 nm	Sol-gel	Nanotubes were fabricated on porous aluminum oxide membranes	NO_2, CH_3OH (0.2 μmol/mol, 2 μmol/mol, 20 μmol/mol) Temperature = 200°C RH = dry air	Gerlitz et al. [18]
PdO loaded SnO_2 (nano-composites)	Size: 7–12 nm	Reverse-Micelle method	Screen-Printing Method	CO Temperature = 300 °C RH = NR*	Yuasa et al. [69]
TiO_2-CeO_2	Ave grain size: 17 nm–28 nm	Sol–gel	NR*	CO (25–400 ppm) Temperature = 200 °C RH 30%	Mohammadi and Fray [40]
SnO_2	NR*	Flame aerosol reactor system	(Immediate power down) IPD mechanism	Ethanol vapor (100 ppm) Temperature = 250 °C RH = NR*	Zhan et al. [71]
Pt-TiO_2 (0.1–0.5 mol%)	NR*	NR*	Screen-printing	H_2, O_2 Temperature = 500 °C–800 °C	Zhang et al. [72]
TiO_2	Particle size: 7 nm–10 nm	Sol–gel	Dip-coating method	NH_3 (56 ppm, 103 ppm, 156 ppm with changing background concentration of NO) Temperature = 350 °C RH = NR*	Biskupski et al. [6]
TiO_2 nanotubes	NR*	NR*	Electrochemical anodization process	Formaldehyde (10–50 ppm) Room temperature RH = ~40%	Shiwai et al. [52]
CuO	29 nm	Spray pyrolysis	NR*	H_2S (250 °C)	Bari et al. [2]
NiO	NR*	Chemical deposition and pyrolysis process	NR*	Benzaldehyde	Yang et al. [68]
In_2O_3	NR*	Film is grown by molecular beam epitaxy (MBE)	NR*	Ozone	Rombach et al. [49]

(*continued on next page*)

Table 5 (*continued*)

Nano particles	Properties of Nanoparticles	Synthesis Technique	Fabrication Technology	Sensing Gas	Author
In2O3	NR*	NR*	NR*	NO_2 (50 ppb) 130 °C	Gonzalez et al. [19]

* NR = Not Reported.
** RH = Relative Humidity.

Acknowledgements

The Author would like to thank Dr. G. Venkatachalam [Professor Emeritus (Adjunct), MPSTME] for critically reviewing the manuscript of this review paper. I would also like to acknowledge the management of NMIMS-MPSTME for their continual support and encouragement.

References

[1] T. Anukunprasert, C. Saiwan, E. Traversa, The development of gas sensor for carbon monoxide monitoring using nanostructure Nb-TiO_2, Sci. Technol. Adv. Mater. 6 (2005) 359–363.
[2] R.H. Bari, S.H. Patil, A.R. Bari, Spray-pyrolized nanostructured CuO thin films for H_2S gas sensor, Int. Nano Lett. (2013) 1–5.
[3] N. Barsan, D. Koziej, U. Weimar, Metal oxide–based gas sensor research: how to? Sens. Actuators B 121 (2007) 18–35.
[4] M. Batzill, U. Deibold, Surface studies of gas sensing metal oxides, PCCP 9 (2007) 2307–2318.
[5] K. Benkstein, S. Semancik, Mesoporous nanoparticle TiO_2 thin films for conductometric gas sensing on micro hot plate platforms, Sens. Actuators B 113 (2006) 445–453.
[6] D. Biskupski, B. Herbig, G. Schottner, R. Moos, Nanosized titania derived from a novel sol–gel process for ammonia gas sensor application, Sens. Actuators B 153 (2011) 329–334.
[7] V.E. Bochenkov, G.B. Sergeev, Metal oxide nanostructures and their applications, in: A. Umar, Y.B. Hahn (Eds.), Metal Oxide Nanoparticles and Their Applications, American Scientific Publication, 2010, pp. 31–52.
[8] X. Chen, S.S. Mao, Titanium Oxide nanomaterials: synthesis, properties, modifications, and applications, Chem. Rev. 107 (2007) 2891–2959.
[9] Y.J. Choi, Z. Seeley, A. Bandyopadhyay, S. Bose, S.A. Akbar, Aluminum-doped TiO_2nano-powders for gas sensors, Sens. Actuators B 124 (2007) 111–117.
[10] E. Comini, Metal oxide nano-crystals for gas sensing, Anal. Chem. ACTA 568 (2006) 28–40.
[11] E. Comini, Metal oxide nanowire chemical sensors: innovation and quality of life, Mater. Today 19 (2016) 559–567.
[12] N.G. Deshpande, Y.G. Gudagea, R. Sharmaa, J.C. Vyasb, J.B. Kim, Y.P. Lee, Studies on tin oxide-intercalated polyaniline nanocomposite for ammonia gas sensing applications, Sens. Actuators B 138 (2009) 76–84.
[13] G. Eranna, B.C. Joshi, D.P. Runthala, R.P. Gupta, Oxide materials for development of integrated gas sensors—a comprehensive review, Crit. Rev. Solid State Mater. Sci. 29 (2004) 111–188.
[14] G.F. Fine, L.M. Cavanagh, A. Afonja, R. Binions, Metal oxide semi-conductor gas sensors in environmental monitoring, Sensors 10 (2010) 5469–5502.
[15] M.E. Franke, T.J. Koplin, U. Simon, Metal and metal oxide nanoparticles in chemiresistors: does the nanoscale matters? Small 1 (2006) 36–50.
[16] V. Galstyan, E. Comonia, C. Barattoa, M. Ferronia, N. Polia, G. Fagliaa, E. Bontempi, M. Brisotto, G. Sberveglieri, Two-phase titania nanotube for gas sensing, Procedia Eng. 87 (2014) 176–179.
[17] C. Garzella, E. Comini, C. Frigeri, G. Sberveglieri, TiO_2 thin films by a novel sol–gel processing for gas sensor applications, Sens. Actuators B 68 (2000) 189–196.
[18] R.A. Gerlitz, K.D. Benkstein, D.L. Lahr, J.L. Hertz, C.B. Montgomery, J.E. Bonevich, S. Semancik, M.J. Tarlov, Fabrication and gas sensing performance of parallel assemblies of metal oxide nanotubes supported by porous aluminum oxide membranes, Sens. Actuators B 136 (2009) 257–264.
[19] O. Gonzaleza, S. Rosoa, R. Calaviaa, X. Vilanovaa, E. Llobeta, NO_2 sensing properties of thermally or UV activated In_2O_3 nanooctahedra, Procedia Eng. 120 (2015) 773–776.
[20] M. Graf, A. Gurlo, N. Barsan, U. Weimar, A. Hierlemann, Microfabricated gas sensor systems with sensitive nanocrystalline metal-oxide films, J. Nanopart. Res. 8 (2006) 823–839.
[21] C.H. Han, S.D. Hang, I. Singh, T. Toupance, Micro-bed of nano-crystalline F-doped SnO2 as sensitive hydrogen gas sensor, Sens. Actuators B 109 (2005) 264–269.
[22] S.A. Hooker, Nanotechnology advantages applied in Gas sensor development, in: The Nanoparticles 2002 Conference Proceedings, USA, 2002.
[23] J. Huang, Q. Wan, Gas sensors based on semiconducting metal oxide one-dimentional nanostructures, Sensors 9 (2009) 9903–9924.
[24] C.M. Hung, D.T.T. Le, N.V. Hieu, On-chip growth of semiconductor metal oxide nanowires for gas sensors: a review, J. Sci.: Adv. Mater. Devices 2 (2017) 262–285.
[25] S. Kanan, O.M. El-Kadri, I.A. Abu-Yousef, M.C. Kanan, Semiconducting metal oxide based sensors for selective gas pollutant detection, Sensors 9 (2009) 8158–8196.
[26] B. Karunagaran, P. Uthirakumar, S.J. Chung, S. Velumani, E.K. Suh, TiO_2 thin film gas sensor for monitoring ammonia, Mater. Charact. 58 (2007) 680–684.
[27] N. Kaura, E. Cominia, N. Polia, D. Zappaa, G. Sberveglieria, Nickel oxide nanowires growth by VLS technique for gas sensing application, Procedia Eng. 120 (2015) 760–763.
[28] T. Kida, A. Nishiyama, M. Yuasa, K. Shimaneo, N. Yamazoe, Highly sensitive NO2 sensors using lamellar-structured WO3 particles prepared by an acidification method, Sens. Actuators B: Chemical 135 (2009) 568–574.
[29] G. Korotcenkov, Metal oxides for solid-state gas sensors: What determines our choice? Mater. Sci. Eng. B 139 (2007) 1–23.
[30] G. Korotcenkov, B.K. Cho, Metal oxide composites in conductometric gas sensors: achievements and challenges, Sens. Actuators B 244 (2017) 182–210.
[31] J. Krainera, M. Delucaa, E. Lacknera, R.W. Teubenbachera, F. Sosadaa, C. Gspanb, K. Rohracherc, E. Wachmannc, A. Koecka, CMOS integrated tungsten oxide nanowire networks for ppb-level H2S sensing, Procedia Eng. 168 (2016) 272–275.
[32] S.A. Krutovertsev, S.I. Sorokin, A.V. Zorin, Y.A. Letuchy, O.Y. Antonova, Polymer film-based sensors for ammonia detection, Sens. Actuators B 7 (1992) 492–494.
[33] E.R. Leite, A.P. Maciel, I.T. Weber, P.N.L. Filho, E. Longo, C.O.P. Santos, A.V.C. Andrade, C.A. Pakoscimas, Y. Maniette, W.H. Schreiner, Development of metal oxide nanoparticles with high stability against particle growth using a metastable solid solution, Adv. Mater. 14 (2002) 905–908.
[34] Y. Li, J. Liang, Z. Tao, J. Chen, CuO particles and plates: synthesis and gas-sensor application, Mater. Res. Bull. 43 (2008) 2380–2385.
[35] X. Liu, S. Cheng, H. Liu, S. Hu, D. Zhang, H. Ning, A survey on gas sensing technology, Sensor 12 (2012) 9635–9665.
[36] E. Llobet, P. Ivanov, X. Vilanova, J. Brezmes, J. Hubalek, K. Malysz, I. Gracia, C. Cane, C. Correig, Screen-printed nanoparticle tin oxide films for high-yield sensor Microsystems, Sens. Actuators B 96 (2003) 94–104.
[37] A.P. Maciel, P.N.L. Filho, E.R. Leite, C.O. Santos, W.H. Schreiner, Y. Maniette, E. Longo, Microstructural and morphological analysis of pure and Ce-doped tin dioxide nanoparticles, J. Eur. Ceram. Soc. 23 (2003) 707–713.
[38] L. Madler, A. Roessler, S.E. Pratsinis, T. Sahm, A. Gurlo, N. Barsan, U. Weimar, Direct formation of highly porous gas sensing films by in situ thermophoretic deposition of flame-made pt/SnO_2 nanoparticles, Sens. Actuators B 114 (2006) 283–295.
[39] G.K. Mani, J.B.B. Rayappan, A highly selective and wide range ammonia sensor—nanostructured ZnO: Co thin film, Mater. Sci. Eng., B 191 (2015) 41–50.
[40] M.R. Mohammadi, D.J. Fray, Nanostructured TiO_2–CeO_2 mixed oxides by an aqueous sol–gel process: Effect of Ce: Ti molar ratio on physical and sensing properties, Sens. Actuators B 150 (2010) 631–640.
[41] B.C. Mohanti, J.W. Lee, D.H. Yeon, Y.H. Jo, J.H. Kim, Y.S. Cho, Dopant induced variations in microstructure and optical properties of CeO_2 nanoparticles, Mater. Res. Bull. 46 (2011) 875–883.
[42] P.T. Moseley, Materials selection for semiconductor gas sensors, Sens. Actuators B 6 (1992) 149–156.
[43] P.T. Moseley, Progress in the development of semiconducting metal oxide gas sensors: a review, Meas. Sci. Technol. 28 (2017) 1–15.
[44] S. Park, S. Kim, G.J. Sun, W.I. Lee, K.K. Kim, C. Lee, Fabrication and NO_2 gas sensing performance of TeO2-core/CuO-shell heterostructure nanorod sensors, Nanoscale Res. Lett. (2014) 1–7.
[45] S.J. Patil, A.V. Patil, V.G. Dighavkar, K.S. Thakare, R.Y. Borase, S.J. Nandre, N.G. Deshpande, R.R. Ahire, Semiconductor metal oxide compounds based gas sensors: a literature review, Front. Mater. Sci. 9 (2015) 14–37.
[46] A.K. Prasad, D.J. Kubinskib, P.I. Gouma, Comparison of sol-gel and ion beam deposited MoO_3 thin film gas sensors for selective ammonia detection, Sens. Actuators B 93 (2003) 25–30.
[47] R. Rella, J. Spadavecchia, M.G. Manera, S. Capone, A. Taurino, M. Martino, A.P. Caricato, T. Tunno, Acetone and ethanol solid-state gas sensors based on TiO_2 nanoparticles thin film deposited by matrix assisted pulsed laser evaporation, Sens. Actuators B 127 (2007) 426–431.
[48] M. Righettoni, A. Amann, S.E. Pratsinis, Breath analysis by nanostructured metal oxides as chemo-resistive gas sensors, Mater. Today 18 (2015) 163–171.
[49] Rombacha,J., Bierwagena, O.,Papadogiannia, A., Mischob, M., Cimallab, V., Bertholdc, T.
[50] A. Ruiz, J. Arbiol, A. Cirera, A. Cornet, J.R. Morante, Surface activation by pt-nanoclusters on titania for gas sensing applications, Mater. Sci. Eng. C 19 (2002) 105–109.
[51] T. Sahm, L. Madler, A. Gularo, N. Barsan, S.E. Patsinis, U. Weimar, Flame spray synthesis of tin dioxide nanoparticles for gas sensing, Sens. Actuators B 98 (2004) 148–153.
[52] L. Shiwai, D. Li, J. Wu, X. Li, S.A. Akbar, A selective room temperature formaldehyde gas sensors using TiO_2 nanotubes array, Sens. Actuators B 156 (2011) 505–509.
[53] R.A. Slepetys, P.A. Vaughan, Solid solution of aluminum oxide in rutile titanium dioxide, J. Phys. Chem. 73 (1969) 2157–2162.
[54] D.M. Smyth, The effects of dopants on the properties of metal oxides, Solid State 129 (2000) 5–12.

[55] Y.F. Sun, S.B. Liu, F.L. Meng, J.Y. Liu, L.T. Kong, J.H. Liu, Metal oxides nanostructures and their gas sensing properties: a review, Sensors 12 (2012) 2610–2631.
[56] H. Tai, Y. Jiang, G. Xie, J. Yu, X. Chen, Z. Ying, Influence of polymerization temperature on NH_3 response of PANI/TiO_2 thin film gas sensor, Sens. Actuators B 129 (2007) 319–326.
[57] A. Teleki, S.E. Pratsinis, K. Kalyanasundaram, P.I. Gauma, Sensing of organic vapors by flame made TiO_2 nanoparticles, Sens. Actuators B 119 (2006) 683–690.
[58] T. Tesfamichael, M. Arita, T. Bostrom, J. Bell, Thin film deposition and characterization of pure and iron-doped electron-beam evaporated tungsten oxide for gas sensors, Thin Solid Films 518 (2010) 4791–4797.
[59] B. Timmer, W. Olthuis, A.V.D. Berg, Ammonia sensors and their application – a review, Sens. Actuators B 107 (2005) 666–677.
[60] A. Trinchi, Y.X. Li, W. Wlodarski, S. Kaciulis, L. Pandolfi, S. Viticoli, E. Comini, G. Sberveglieri, Investigation of sol-gel prepared CeO_2-TiO_2 thin films for oxygen gas sensing, Sens. Actuators B 95 (2003) 145–150.
[61] A. Umar, A.A. Alshahrani, H.A.R. Kumard, CuO nanosheets as potential scaffolds for gas sensing applications, Sens. Actuators B 250 (2017) 24–31.
[62] G. Velmathi, S. Mohan, R. Henry, Analysis and review of tin oxide-based chemoresistive gas sensor, IETE Tech. Rev. (2015) 1–9.
[63] C. Wang, L. Yin, L. Zhang, D. Xiang, R. Gao, Metal oxide gas sensors: sensitivity and influencing factors, Sensors 10 (2010) 2088–2106.
[64] S. Wendt, R. Schaub, J. Matthiesen, K.V. Vestergaard, E. Wahlstrom, M.D. Rasmussen, P. Thostrup, L.M. Molina, E. Laesgaard, I. Stensgaard, B. Hammer, F. Besenbacher, Oxygen vacancies on TiO_2 (110) and their interaction with H_2O and O_2: a combined high-resolution STM and DFT study, Surf. Sci. 598 (2005) 226–245.
[65] K. Wetchakun, T. Samerjai, N. Tamaekong, C. Liewhiran, C. Siriwong, V. Kruefu, A. Tuantranont, S. Phanichphant, A. Wisitsoraat, Semiconducting metal oxides as sensors for environmentally hazardous gases, Sens. Actuators B 160 (2011) 580–591.
[66] D.E. Williams, Semiconducting oxides as gas-sensitive resistors, Sens. Actuators B 57 (1999) 1–16.
[67] N. Yamazoe, New approaches for improving semiconductor gas sensors, Sens. Actuators B 5 (1991) 7–19.
[68] F. Yang, Z. Guo, Engineering NiO sensitive materials and its ultra-selective detection of benzaldehyde, J. Colloid Interface Sci. 467 (2016) 192–202.
[69] M. Yuasa, T. Masaki, T. Kida, K. Shimanoe, N. Yamazoe, Nanosized PdO loaded SnO_2 nanoparticles by reverse micelle method for highly sensitive CO gas sensor, Sens. Actuators B 136 (2009) 99–104.
[70] D. Zappaa, E. Cominia, G. Sberveglieria, Gas-sensing properties of thermally-oxidized metal oxide nanowires, Procedia Eng. 47 (2012) 430–433.
[71] Z. Zhan, W.N. Wang, L. Zhu, W. An, P. Biswas, Flame aerosol reactor synthesis of nanostructured SnO_2 thin films: high gas sensing properties by control of morphology, Sens. Actuators B 150 (2010) 609–615.
[72] M. Zhang, Z. Yuan, J. Song, C. Zheng, Improvement and mechanism for the fast response of a Pt/TiO_2 gas sensor, Sens. Actuators B 148 (2010) 87–92.